# MAPPING STREET OBSTRUCTIONS IN AN URBAN STR EET ENVIRONMENT USING MLS DATA

Chun Liu[1], Yuanfan Qi[1,*]

[1]College of Surveying and Geo-informatics, Tongji University, Shanghai 200092, China
liuchun@tongji.edu.cn, 2011478@tongji.edu.cn

**Commission II, WG II/10**

**KEY WORDS:** MLS data, street obstruction, non-obstruction space, obstruction analysis, urban street environment.

**ABSTRACT:**
It is crucial to ensure no obstruction above urban streets for drivers. If street obstructions limit the sight of drivers, it may reduce the ability of drivers to perceive the surrounding road conditions. Street obstructions are usually caused by a variety of different factors. It includes street trees overgrowing into the space above the road or the wrong placement of the infrastructure. To ensure road traffic safety, transportation agencies are required to obtain the existence of street obstructions. To address the issue, this paper proposes a novel method to detect street obstructions. The method consists of two main steps: non-obstruction space construction by the Alpha-Smooth method and street obstruction analysis. The proposed approach is able to map the thematic map of street obstructions in the urban environment. The algorithm was tested on urban streets in Shanghai, China, and successfully obtained obstructions information. The results indicated that street trees are the main components of road obstructions. The proposed approach can make contribution to street maintenance and obstructions monitoring that aim to develop safer urban street environments.

## 1. INTRODUCTION

### 1.1 Background

Street obstruction in the urban environment may lead to driver's delayed or no observation of traffic conditions; thus, to ensure traffic safety, regular inspection of street obstructions is one of the basic tasks of city management. However, with the development of cities, plenty of urban infrastructures, such as street trees, shrubs, billboards, have been renovated or newly built, resulting in overgrowing into the space above the road and untimely obstruction detection. Unfortunately, current studies fail to sufficiently account for these obstructions in the street environment (Gayah et al., 2015). Detecting and mapping street obstructions accurately is an urgent issue, which is the main focus of our paper.

Generally, the existing obstruction detection methods can be categorized into two groups: 1) manual; and 2) automated. In manual methods, investigators will visually identify obstructions in the field. Although manual methods can essentially meet the needs of city management, it is time-consuming and workforce. In addition, visual discrimination is often difficult to have high accuracy, thus failing to satisfy the demand of the high-density city. The latter is automatic methods, namely, detecting and mapping street obstructions from measurement data. Compared with manual methods, automated methods significantly save cost and time. Furthermore, in recent years, the mobile laser scanning (MLS) system has become one of the most convenient tools in road environment (Li et al., 2016) because the MLS system can obtain accurate 3D road information efficiently and provides a full-view perspective of the road scene (Yadav et al., 2018a; Yadav et al., 2018b).

Therefore, this paper focuses on automatically detecting and mapping street obstructions for urban infrastructure maintenance. Although the topic of obstruction detection from MLS data has been studied by previous researchers, two main challenges still need to be considered and discussed. First, a non-obstruction space issue, that is, due to the complex topology of the urban road network, how to define a three-dimensional space without obstructions and consistent with road network structure? Second, the obstruction refinement challenge, as vehicles and pedestrians are widely distributed on the road, which brings difficulties to obstruction detection.

### 1.2 Related Works

Over the last decade, various methods for street obstruction detection and analysis have been developed. In this section, we will briefly discuss previous related works.

As sight distance is a critical geometric element to road safety, many methods, such as the voxel-based (Shalkamy et al., 2020), the GIS-based (Castro. et al., 2014), and the DEM-based (Castro et al., 2016), have been applied to analyze the obstruction based on the sight. For example, Ma combined cylindrical perspective projection with modified Delaunay triangulation (Ma et al., 2019). All point clouds in the cone of vision of the driver were projected onto the same flat plane to determine whether these objects were obstructions that would cause occlusion. This method can visually check the location by simulating the driver's dynamic vision along the highway. González-Gómez firstly obtained the slight distance from the LiDAR retrieved data. Then, the 3D road models derived from the LiDAR retrieved data were employed to obtain the available sight distances. Finally, after comparing the required with the available visibility, obstructions that might affect visibility, such as vegetation, traffic, or furniture, were evaluated (González-Gómez et al., 2021). However, it was developed to assess conflicts along intersections rather than urban streets. In Gargoum's research, the sight assessment was composed of two main steps (Gargoum and Karsten, 2021). The first step was analyzing visibility between multiple observers and target points, and the limitations along the highway were thus identified. The second phase of the process involved extracting and classifying the obstruction. The method presented a descriptor for the 3D distribution of points in the neighborhood to identify obstructions along each sight line by constructing sight lines between observers and targets while it was designed for highways only.

* Corresponding author

However, the main problem of these sight-based methods for obstruction detection is that they are often set up for a particular scene and do not apply to the common urban street environment. In recent years, visibility-based methods have been applied in urban street environments for obstruction detection. In the following, we will review visibility-based approaches.

Due to no requirement of preprocessing in raw point clouds, the hidden point removal (HPR) operator by Katz (Katz et al., 2007) has been widely used in visibility determination. The hidden point removal operator is a method to generate 2.5D views from 3D point clouds. It can determine the visible points with no need for reconstructing a surface or estimating normals, which greatly reduces computational complexity. Mehra (Mehra. et al., 2010) improved the HPR operator using a graph-based approximation algorithm. By collating the partial connectivity information from multiple visibility queries, the developed robust HPR operator can reduce the influence of noise content. Huang (Huang et al., 2017) attempted to carry out the HPR operator to obtain obstructions blocking the traffic sign. The viewpoints were estimated from the trajectory data, then the topological observation relationship between viewpoint and traffic sign was established. By applying the operator to the road scene, obstructions were calculated from the corresponding viewpoint. Rozsa (Rozsa and Sziranyi, 2018) adopted the HPR operator in obstruction analysis of automatic vehicles. Moreover, Zhao (Zhao et al., 2020) focused on the influence of obstructions on the visibility of urban road environments based on 3D voxels and volume index generated from MLS data. In his method, the MLS data was converted into voxelization firstly. Next, the ray-triangle intersection was adopted to calculate the intersection points between sights and voxels were calculated. Finally, the volume index was obtained to describe the visibility of different urban street environments. However, his method did not give the exact location of the obstructions needing maintenance.

Moreover, in recent years, deep learning technology has been used to estimate street obstructions, which can achieve a comprehensive understanding of urban road visibility. Ma (Ma et al., 2022) put forward a virtual scanning method to understand sight obstacles. The virtual scanning method was derived by deep neural networks trained on semanticKITTI, which help detect street obstacles and poor-visibility locations. Liu (Liu et al., 2020) proposed an SP-ICNet model based on feature fusion to can realize obstruction detection naturally, which can avoid large computation and memory consumption by capturing contextual information. Fang (Fang et al., 2020) developed an annotated data generation framework to train DNNs models and then extracted obstructions' position and orientation based on the learned obstacle distribution. Ye (Ye et al., 2021) proposed a novel lightweight end-to-end network to locate obstructions in real-time and all-weather conditions, but it was constructed for railways only.

In summary, although the sight-based street obstruction analysis has been extensively researched in the past few years, they are often only designed for special situations such as intersections or highways. In addition, visibility-based methods are often involved with the selection of viewpoints, which contribute the computational complexity. Therefore, obtaining the street obstructions of urban street environments from MLS point clouds remains an ongoing problem.

### 1.3 Our Works

In this paper, an obstruction detection method is proposed. More specifically, a novel concept of non-obstruction space is proposed, it defines the three-dimensional space without obstructions based on the road topology and traffic rules, and then non-ground objects in this non-obstruction space are detected. Particularly, vehicles and pedestrians are removed from the detected obstruction according to their geometrical features and physical features. The main contributions are summarized as follows:

(1) The Alpha-Smooth method is proposed to extract road boundaries and improve the reliability of non-obstruction space.
(2) Street obstruction analysis method is given for street obstruction detection and refinement.
(3) A thematic map of street obstruction is drawn for the urban road management and greening departments.

## 2. METHODOLOGY

### 2.1 Overview

The proposed method is comprised of three parts (Fig. 1): data preprocessing, non-obstruction space construction based on the Alpha-Smooth method, and obstruction detection analysis.

It is assumed that the preprocessed results of MLS point clouds are provided in advance. Because the main task of our paper is detecting and mapping street obstruction in the street environment, the preprocessing step is described briefly in the following.

MLS point clouds in urban scenes contain many objects, such as street trees, bushes, buildings, poles, ground, which contribute to the difficulty of obstruction detection. Therefore, MLS point clouds are firstly divided into ground points and non-ground points, non-ground points are prepared for obstruction detection. On this basis, the road surfaces are extracted according to the geometric mutation of the road edge. Specifically, height difference, plane distance, space distance, and slope between adjacent points on scan lines are calculated. The road surface is roughly extracted from the ground points through the sudden change of geometric attributes between the road surface and the surrounding object.

However, non-ground objects also include pedestrians and vehicles on the road, which need to be removed from non-ground points for obstruction detection. Moreover, road boundaries are discontinuous due to the block of the car. To address these problems, the boundary is detected and refined from the road surface. Finally, the obstruction analysis model is applied to obtain obstructions and map their information.

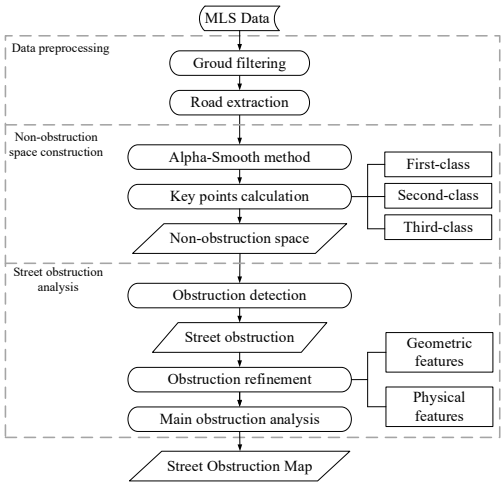


**Figure 1**. Flowchart of the proposed method.

### 2.2 Non-obstruction Space Construction

According to the concept of construction clearance put forward by the Ministry of Transport of the People's Republic of China, the cross-section of the road surface shall be free from any obstruction. Thus, we propose our concept of non-obstruction space. It is a three-dimensional continuous space without any obstructions. The spatial geometry is determined by the traffic standard and the shape of the road network. This section will construct the non-obstruction space, and three key points are calculated to construct the 3D non-obstruction space.

**2.2.1 The Alpha-Smooth method:** After data preprocessing, although the extracted road surface can approximately represent the bottom plane of the non-obstruction space, its shape and the large number of road surface points make it difficult to represent the non-obstruction space by road directly. Therefore, the road boundary is applied to delineate the fit geometry of the road. Thus the Alpha-Smooth method based on the Alpha-shapes and the smooth curve is proposed to extract and refine the road boundary.

The concept of alpha shape was put forward in 1983 to define the shape of a point set on a plane (Edelsbrunner et al., 1983). The alpha shape is a series of simple curves and has been widely applied in the outline extraction of the data point on the Euclidean plane (Wu et al., 2015). Fig. 2a shows the example of the alpha shapes algorithm run in a ball-rolling way. To delete the fake boundary points caused by vehicles occlusions, the density-based spatial clustering of applications with noise (DBSCAN) is used to divide the boundary into different parts (Fig. 2b). Then curvature in each part is calculated, if the curvature changes suddenly, this part is considered as the fake boundary points and thus deleted (Fig. 2c).

The next step is to add the boundary points occluded by vehicles, and smooth curves are used to fit road boundaries in this section. When there is a tangent at every point on the curve, and the tangent rotates continuously with the movement of the tangent point, such a curve is called a smooth curve. Curve fitting is commonly applied in the reconstruction of curves from measured points because smooth curve fitting can control both the accuracy and the fairness of the fitted curve (Ueng et al., 2006). Due to the regular road, the smooth curves are used to add the boundary points or close the gap (Fig. 2d).

**2.2.2 Key Points Calculation:** In general, the construction clearance is a polygon close to the road surface, and each construction clearance is composed of six points. These points are classified into three categories based on the elevation. First-class points ($FCp$) are sampled directly from the road boundary every box width ($BW$), and other points in second class and third class are calculated as follow:

$$SCp = FSp + H1 \times nv \tag{1}$$

$$TCp = FSp - E + H2 \times nv \tag{2}$$

Where $FCp$, $SCp$, *and* $TCp$ are first-class points, second-class points, and third-class points, respectively. $nv$ is the normal vector of the ground point near first-class points. $H1$, $H2$, and $E$ are determined by the traffic standard.

As Shown in Fig. 3, the points of the two sections are connected into a non-obstruction box ($NOB$). Furthermore, multiple non-obstruction boxes combine to form the non-obstruction space ( $NOS$ ). Thus, the non-obstruction space we proposed is expressed as follows:

$$NOS = \{NOB_i | i = 1,2 \dots N\} \tag{3}$$

Where N is the number of non-obstruction boxes.

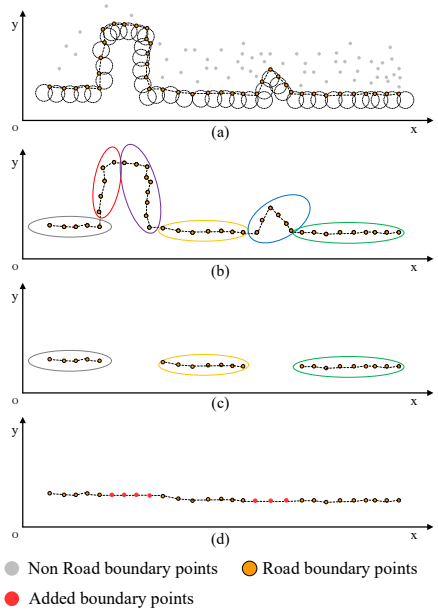


**Figure 2.** Sketch of Alpha-Smooth method: (a) The application of alpha shapes, (b) Several parts labeled by DBSCAN, (c) Deletion of non-boundary points, (d) Refined road boundary points after smooth curve fitting.

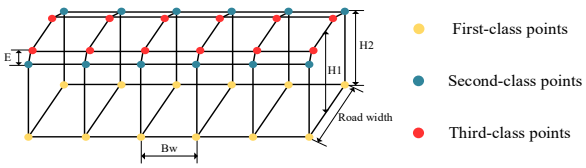


**Figure 3.** Sketch of non-obstruction space construction: multiple boxes form the non-obstruction space.

### 2.3 Street Obstruction Analysis

The non-obstruction space derived from MLS data is presented in subsection 2.2, which represents the three-dimensional space without any obstruction. In this section, street obstruction analysis will be conducted. Trees are extracted from non-objects for the main obstruction analysis (Fig. 4b), the non-objects within the non-obstruction space are detected (Fig. 4c), then vehicles and pedestrians are removed (Fig. 4d).

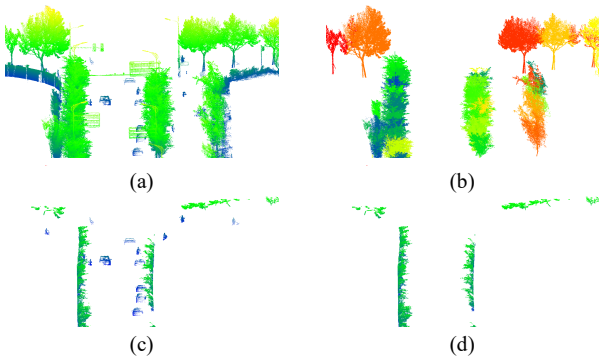


**Figure 4.** General overview of street obstruction analysis: (a) Non-ground objects, (b) Street tree extraction, (c) Obstruction detection, (d) Obstruction refinement.

**2.3.1 Obstruction Detection:** Since non-obstruction space is the collection of non-obstruction boxes, the first step involves traversing all the boxes and calculating all non-ground points in the non-obstruction boxes.

To be more specific, for each non-obstruction box, the Axis-aligned bounding box (AABB) of each box is obtained according to the three-class points that constitute each box firstly. Then point clouds within the AABB are filtered to reduce computing costs.

Next, the topological relationship between the point and the non-obstruction box should be determined. Here, we adopt the ray-based method. Briefly, a ray is introduced to intersect the box at a point. If the number of intersections is odd, the point is inside the box. Otherwise, it is outside the box. The ray-triangle intersection method is applied to compute every intersection of each triangle with the ray. Each box has eight facets, and each facet can be decomposed into two triangles. Thus, a box has 16 triangles. Finally, the algorithm introduced by Möller is applied to solve the intersection of a line and triangle mathematically (Möller and Trumbore, 1997).

As shown in Fig. 5, $T(u,v)$ is the intersection point between the triangle $(V_0, V_1, V_2)$ and the ray $\vec{D}$. $P$ is the point within AABB corresponding to each box. The point $T(u,v)$ is calculated with Eq. (4):

$$T(u,v) = (1-u-v)V_0 + uV_1 + vV_2 \quad (4)$$

Where $(u,v)$ are the barycentric coordinates, which must fulfill $u > 0$, $v > 0$, and $u + v \leq 1$.

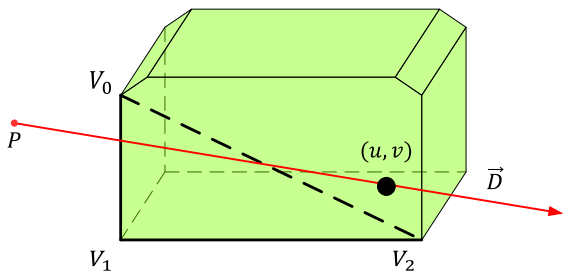


**Figure 5.** The intersection between a ray and a non-obstruction box.

**2.3.2 Obstruction Refinement:** Many non-obstructions such as vehicles and pedestrians are mistaken as the detected obstruction as mentioned in subsection 2.3. Therefore, the geometrical features and physical features of non-ground objects are used to delete these vehicles and pedestrians. The specific steps of the obstruction refinement algorithm are as follows:

(1) Euclidean clustering algorithm is used to cluster obstruction into point clouds clusters based on the Euclidean distance. The centroid of each cluster is set as $C_i$.

(2) Count the number $n_i$ of points in each cluster. The clusters that satisfy Equation (5) will be put into set $ClusterSet\_n_i$. The parameter $n_t$ in this paper is set as 20.

$$n_i > n_t \quad (5)$$

(3) Calculate the distance $D_i$ from the centroid point $C_i$ of each cluster to the road boundary line of the set $ClusterSet\_n_i$. The clusters that satisfy Equation (6) are named as $ClusterSet\_d_i$. The parameter $d_t$ in this paper is set as 2.5.

$$D_i < d_t \quad (6)$$

(4) Calculate the distance $H_i$ from the centroid point $C_i$ of each cluster to the road surface of the set $ClusterSet\_d_i$. The clusters that satisfy Equation (7) are named as $ClusterSet\_h_i$. The parameter $h_t$ in this paper is set as 1.5.

$$H_i > h_t \quad (7)$$

(5) Repeat the above steps until all of the clusters have been processed and the clusters $ClusterSet\_h_i$ are point clouds that encroach on the non-obstruction space.

## 3. CASE STUDY

### 3.1 Case Data

The case area is 6.4 km long and covers an area of 751,000$m^2$, and the height difference between the two ends of the road is about 8.3m. The case area represents a typical urban scene with a high-density road network. The road network is complex with curved roads, and the road width varies in different sections. Vehicles are parked on both sides. Furthermore, the case area contains straight lanes, intersections, three forks, and other roads. All of the above characteristics lead to difficulties in street obstruction analysis and mapping.

On 10 October 2018, the point cloud data in Pudong New District Shanghai, China, were collected using the mobile laser measurement system. The total number of laser points in the case area is 384,502,295. The location and point clouds sketch of the case area are shown in Fig. 6.

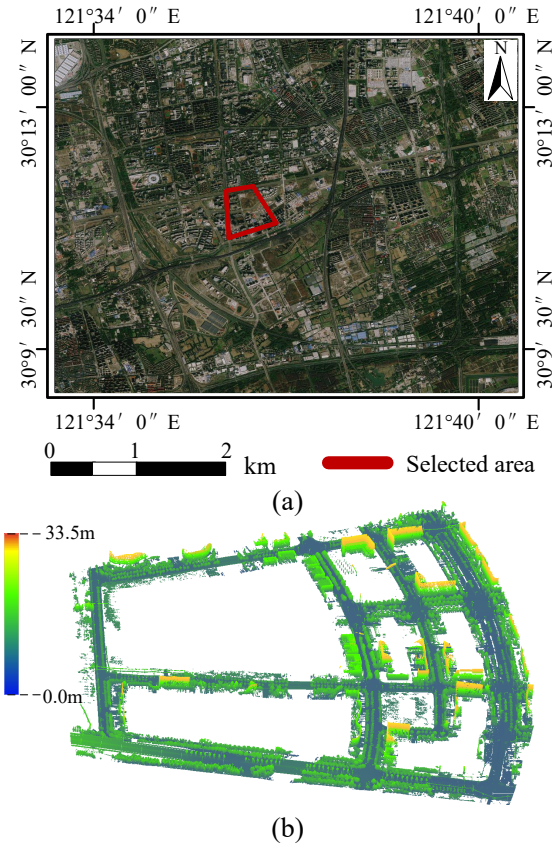


**Figure 6.** Sketch of the case area: (a) Location of the case area, (b) MLS point clouds.

### 3.2 Parameter selection

The experimental parameters are selected as follows. As previously described in subsection 2.2.2, the parameter $BW$ should be set to make the non-obstruction space as similar to the road as possible, thus $BW$ is generally set to 2.0m. From experience, $n_t$ is closely related to the density of the MLS data, it is set to 20. The parameter $d_t$ and $h_t$ are set to exclude vehicles and pedestrians away from the road boundary and close to the road, respectively. The values of these parameters are listed in Table 1.

| Parameter | Value |
|---|---|
| $BW$ | 2.0m |
| $n_t$ | 20 |
| $d_t$ | 2.5m |
| $h_t$ | 1.5m |

**Table 1**. Parameter setting in this paper.

### 3.3 Non-obstruction Space Construction Results

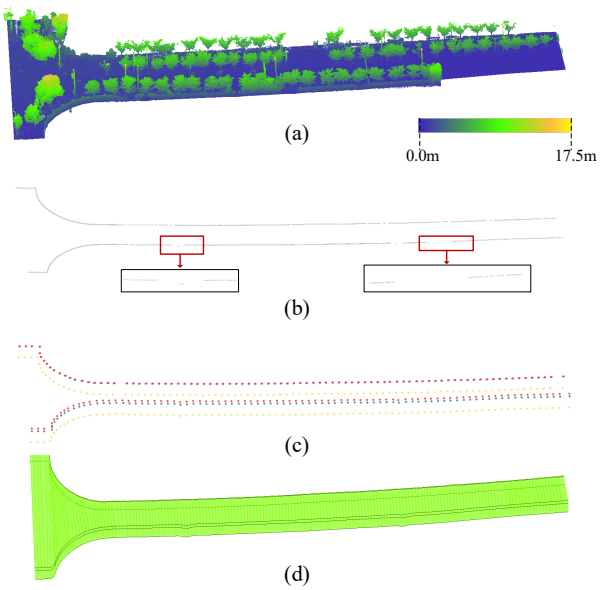


**Figure 7.** Non-obstruction space construction example: (a) Raw MLS data, (b) Road boundary, (c) Key points, (d) Non-obstruction space.

In this section, a typical road is taken as an example to display the detailed non-obstruction space construction process (shown in Fig. 7). Next, the whole non-obstruction space of the whole case area is given in Fig.8.

Based on the Alpha-Smooth method, the road boundary line is extracted and refined from the original point cloud (Fig. 7a). Then, three class points are calculated according to the road boundary and traffic standard. Finally, multiple boxes form the non-obstruction space in turn. It can be seen that although the extracted road boundary (Fig. 7b) is missing, continuous key points (Fig. 7c) can still be formed according to this method.

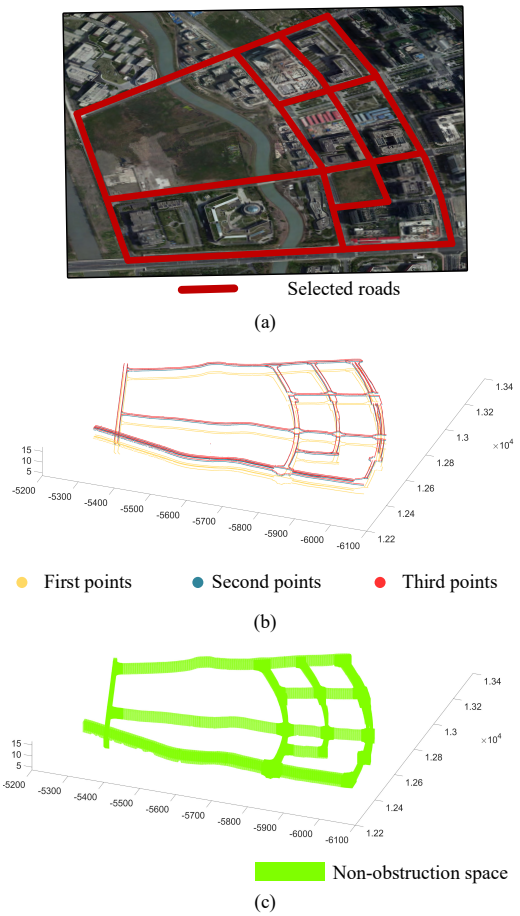


**Figure 8.** Non-obstruction space of the case area: (a) Selected roads, (b) Three class points, (c) Non-obstruction space.

Fig. 8(a-c) shows the selected roads, three class points, and non-obstruction for the case area, respectively. As we can see from the case area, first-class points originate from the road boundary and thus are farther apart from points of the second and third class points, while points of the second and third class are near. In addition, the overall trend of the non-obstruction space and road network is similar, and the non-obstruction space is continuous.

### 3.4 Street Obstruction Analysis Results

The non-obstruction space has been constructed in subsection 3.3. To obtain street obstructions information, non-ground objects are detected within the non-obstruction space, then a thematic map of street obstruction is drawn for the urban management department.

In this section, two scenes are taken as examples to display the detailed street obstruction detected results. Fig. 9(a, c) shows the distribution of non-obstruction space in the street environment, and Fig. 9(b, d) shows the obstruction detection results. Scene I shows the obstruction detection results in a T-junction. As shown in Fig. 9(a), the non-obstruction space is above the road. The obstruction detection result shows that the obstructions occupying the space are mainly street trees and bushes. Scene II is an intersection; thus, the non-obstruction space is also crisscrossed. The objects that occupy space in scene 2 are also mainly street trees.

This contribution has been peer-reviewed. The double-blind peer-review was conducted on the basis of the full paper.
https://doi.org/10.5194/isprs-annals-V-2-2022-375-2022 | © Author(s) 2022. CC BY 4.0 License.

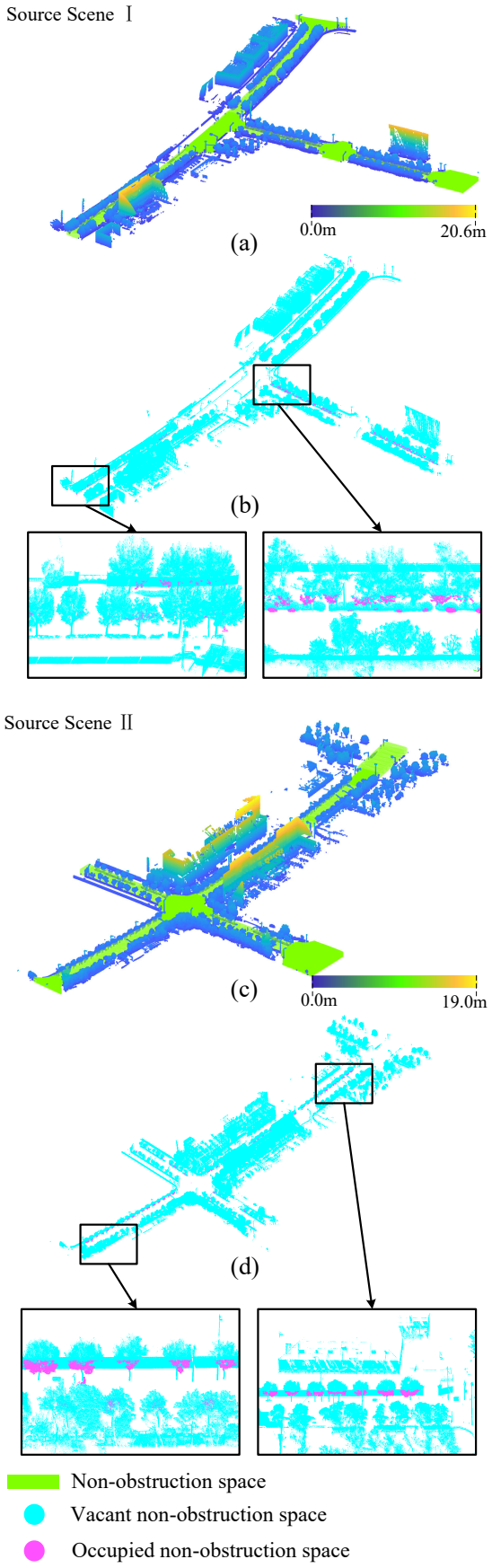


**Figure 9.** Examples of street obstruction analysis results: (a, c) The non-obstruction space of two scenes, (b, d) Obstructions detection results of two scenes.

As an important part of urban infrastructure (Li et al., 2021a), the street tree plays a crucial role in many aspects. Due to the rapid growth of street trees, street trees often need to be trimmed in time. Therefore, we identify street trees as key obstructions for analysis. Here, a branch-trunk-constrained hierarchical clustering method (Li et al., 2021b) for street trees extraction is used. After calculation, street trees account for 94.8% of all obstruction point clouds, and the remaining obstructions are bush, billboards, and so forth. The results show that street trees are the main components of road obstructions.

In order to help the city management department achieve accurate removal of street obstructions, a thematic map of street obstruction maintenance information is drawn. As shown in Fig. 10, grey areas are roads, yellow areas are the building facades, green areas are main tree obstructions, and red areas are other obstructions. All street obstructions are located on both sides of the road, and most of them are near the straight road, with few obstructions around the viaduct (the leftmost road). The obstructions that occupy most space are street trees, perhaps because they grow too fast to be pruned. This situation reminds the greening department of timely maintenance of street trees. Our thematic map also provides the corresponding obstruction information for the maintenance personnel.

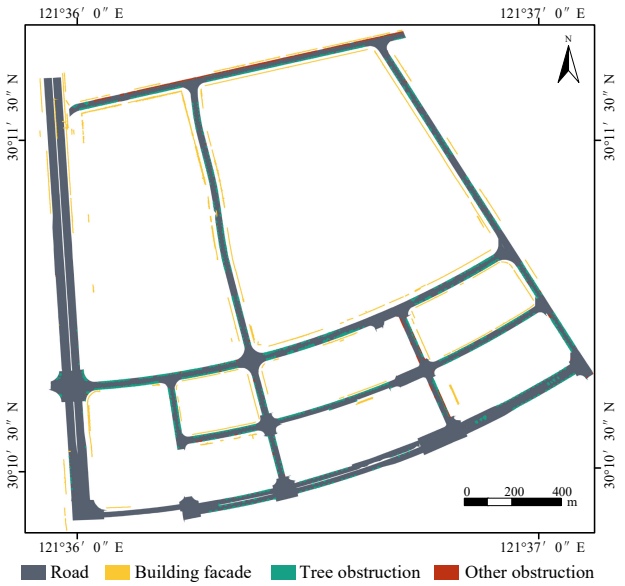


**Figure 10.** Thematic map of street obstructions.

### 3.5 Comparison result

To verify the effect of our method, our method is compared with Luoma's method (Luoma et al., 2015). In Luoma's method, the obstruction is determined by comparing the height of the object with the street lamp. If the object is higher than the street lamp nearby, it is considered an obstruction.

As shown in Fig. 11, red areas are obstructions. It can be seen that Luoma's method regards the two trees as obstacles that need to be removed as a whole, while our method only needs to trim the branches of some trees. In addition, Luoma's method fails to consider the case that the branches of trees will enter the non-obstruction space of the street. Therefore, our method can not only identify the obstructions invading the road but also avoid the overall removal of trees to the maximum, which is of positive significance for urban greening and conservation.

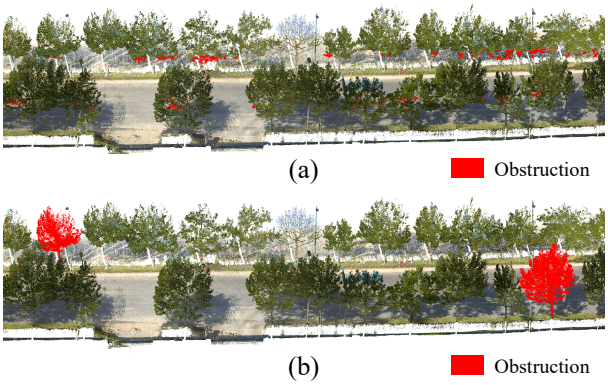


**Figure 11.** Results of different methods: (a) Our method, (b) Luoma's method.

## 4. CONCLUSION

Accurate maintenance of street obstruction is critical for the safety of the urban street environment. In this study, we have presented a new method to detect and map street obstructions intruding over the road. Our obstruction analysis is based on the non-obstruction space generated from MLS data, representing the 3D space without obstruction. Our approach consists of two main steps: non-obstruction space construction by the Alpha-Smooth method and street obstruction analysis. To demonstrate our approach, a typical urban street environment is tested and analyzed. In addition, the thematic map will also provide accurate information for removing urban obstructions.

However, several issues still need to be further studied. Our study only regards objects inside the non-obstruction space as obstructions, without considering obstructions to sight distance. Therefore, in future research, to ensure sufficient sight distance in the street environment, we will extract and detect street obstructions causing sight distance limitations. In addition, because the occlusion of vehicles will inevitably cause the loss of road point clouds, we will use UAV-derived point clouds as a supplement to MLS point clouds.

## ACKNOWLEDGEMENT

This work was supported by the Major Program of the National Natural Science Foundation of China (Grant No. 42130106).

## REFERENCES

Castro, M., Lopez-Cuervo, S., Paréns-González, M., de Santos-Berbel, C., 2016. LIDAR-based roadway and roadside modelling for sight distance studies. *Survey Review,* 48, 309-315.

Castro., M., Anta., J.A., Iglesias., L., S´anchez, J.A., 2014. GIS-Based System for Sight Distance. *ASCE J. Comput. Civil Eng,* 28, 04014005-04014012.

Edelsbrunner, H., Kirkpatrick, D., Seidel, R., 1983. On the Shape of a Set of Points in the Plane. *IEEE TRANSACTIONS ON INFORMATION THEORY,* 29, 551-559.

Fang, J., Zhou, D., Yan, F., Zhao, T., Zhang, F., Ma, Y., Wang, L., Yang, R., 2020. Augmented LiDAR Simulator for Autonomous Driving. *IEEE Robotics and Automation Letters,* 5, 1931-1938.

Gargoum, S.A., Karsten, L., 2021. Virtual assessment of sight distance limitations using LiDAR technology: Automated obstruction detection and classification. *Automation in Construction,* 125, 103579-103592.

Gayah, V.V., Ilgin Guler, S., Gu, W., 2015. On the impact of obstructions on the capacity of nearby signalised intersections. *Transportmetrica B: Transport Dynamics,* 4, 48-67.

González-Gómez, K., López-Cuervo Medina, S., Castro, M., 2021. Assessment of intersection conflicts between riders and pedestrians using a GIS-based framework and portable LiDAR. *GIScience & Remote Sensing,* 58, 587-602.

Huang, P., Cheng, M., Chen, Y., Luo, H., Wang, C., Li, J., 2017. Traffic Sign Occlusion Detection Using Mobile Laser Scanning Point Clouds. *IEEE Transactions on Intelligent Transportation Systems,* 18, 2364-2376.

Katz, S., Tal, A., Basri, R., 2007. Direct visibility of point sets. *ACM Transactions on Graphics,* 26(3), 24-36.

Li, F., Oude Elberink, S., Vosselman, G., 2016. Pole-Like Street Furniture Decompostion in Mobile Laser Scanning Data. *ISPRS Annals of Photogrammetry, Remote Sensing and Spatial Information Sciences,* III-3, 193-200.

Li, J., Cheng, X., Wu, Z., Guo, W., 2021a. An Over-Segmentation-Based Uphill Clustering Method for Individual Trees Extraction in Urban Street Areas From MLS Data. *IEEE Journal of Selected Topics in Applied Earth Observations and Remote Sensing,* 14, 2206-2221.

Li, J., Cheng, X., Xiao, Z., 2021b. A branch-trunk-constrained hierarchical clustering method for street trees individual extraction from mobile laser scanning point clouds. *Measurement,* 189, 110440-110455.

Liu, B., Lv, Y., Gu, Y., Lv, W., 2020. Implementation of a Lightweight Semantic Segmentation Algorithm in Road Obstacle Detection. *Sensors (Basel),* 20, 7089-7103.

Luoma, V., Tanhuanpää, T., Holopainen, M., Vastaranta, M., Ninni Saarinen, V., Kankare, 2015. Allocating tree crown pruning with ALS-data — A case study in the city of Helsinki, *Joint Urban Remote Sensing Event (JURSE)* ,1-4.

Ma, Y., Zheng, Y., Cheng, J., Easa, S., 2019. Real-Time Visualization Method for Estimating 3D Highway Sight Distance Using LiDAR Data. *Journal of Transportation Engineering, Part A: Systems,* 145, 04019006-04019020.

Ma, Y., Zheng, Y., Easa, S., Wong, Y.D., El-Basyouny, K., 2022. Virtual analysis of urban road visibility using mobile laser scanning data and deep learning. *Automation in Construction,* 133, 104014-104060.

Mehra., R., Tripathi., P., Sheffer., A., Mitra., N.J., 2010. Visibility of Noisy Point Cloud Data. *Comput. Graph,* 34(3), 219-230.

Möller, T., Trumbore, B., 1997. Fast, Minimum Storage Ray-Triangle Intersection. *Journal of Graphics Tools,* 2, 21-28.

Rozsa, Z., Sziranyi, T., 2018. Obstacle Prediction for Automated Guided Vehicles Based on Point Clouds Measured by a Tilted

LIDAR Sensor. *IEEE Transactions on Intelligent Transportation Systems,* 19, 2708-2720.

Shalkamy, A., El-Basyouny, K., Xu, H.Y., 2020. Voxel-Based Methodology for Automated 3D Sight Distance Assessment on Highways using Mobile Light Detection and Ranging Data. *Transportation Research Record: Journal of the Transportation Research Board,* 2674, 587-599.

Ueng, W.-D., Lai, J.-Y., Tsai, Y.-C., 2006. Unconstrained and constrained curve fitting for reverse engineering. *The International Journal of Advanced Manufacturing Technology,* 33, 1189-1203.

Wu, B., Yu, B., Huang, C., Wu, Q., Wu, J., 2015. Automated extraction of ground surface along urban roads from mobile laser scanning point clouds. *Remote Sensing Letters,* 7, 170-179.

Yadav, M., Khan, P., Singh, A.K., Lohani, B., 2018a. Generating Gis Database of Street Trees Using Mobile Lidar Data. *ISPRS Annals of Photogrammetry, Remote Sensing and Spatial Information Sciences,* IV-5, 233-237.

Yadav, M., Lohani, B., Singh, A.K., 2018b. Road Surface Detection from Mobile Lidar Data. *ISPRS Annals of the Photogrammetry, Remote Sensing and Spatial Information Sciences,* IV-5, 95-101.

Ye, T., Ren, C., Zhang, X., Zhai, G., Wang, R., 2021. Application of Lightweight Railway Transit Object Detector. *IEEE Transactions on Industrial Electronics,* 68, 10269-10280.

Zhao, Y., Wu, B., Wu, J., Shu, S., Liang, H., Liu, M., Badenko, V., Fedotov, A., Yao, S., Yu, B., 2020. Mapping 3D visibility in an urban street environment from mobile LiDAR point clouds. *GIScience & Remote Sensing,* 57, 797-812.